Selective retina therapy (SRT): A review on methods, techniques, preclinical and first clinical results

BRINKMANN R.[1], *ROIDER J.*[2], *BIRNGRUBER R.*[1]

ABSTRACT

Selective retina therapy (SRT) is a new laser procedure for retinal diseases that are thought to be associated with a degradation of the retinal pigment epithelium (RPE). The aim of the irradiation is to selectively damage the RPE without affecting the neural retina, the photoreceptors and the choroid. Goal of the treatment is to stimulate RPE cell migration and proliferation into the irradiated areas in order to improve the metabolism at the diseased retinal sites. In a pilot study more than 150 patients with soft drusen, retinopathia centralis serosa (RCS) and macular edema were treated. The first 3-center international trial targets diabetic macular edema and branch vein occlusion.

In this review, selective RPE effects are motivated and two modalities to achieve selective RPE effects will be introduced: a pulsed and a continuous wave scanning mode. The mechanism behind selective RPE-effects will be discussed reviewing in vitro results and temperature calculations. So far clinical SRT is performed by applying trains of 30 laser pulses from a Nd:YLF-Laser (527 nm, 1.7 μs, 100 Hz) to the diseased fundus areas. In the range of 450-800 mJ/cm^2 per pulse, RPE-defects in patients were proved angiographically by fluorescein or ICG-leakage. The selectivity with respect to surrounding highly sensitive tissue and the safety range of the treatment will be reviewed. With the laser parameters used neither bleeding nor scotoma, proved by microperimetry, were observed thus demonstrating no adverse effects to the choroid and the photoreceptors, respectively.

During and after irradiation, it shows that the irradiated locations are ophthalmoscopically invisible, since the effects are very limited and confined to the RPE, thus a dosimetry control is demanded. We report on a non-invasive opto-acoustic on-line technique to monitor successful RPE-irradiation and compare the data to those achieved with standard angiography one-hour post treatment.

KEYWORDS

Selective treatment, RPE, μs-pulses, on-line dosimetry, laser scanner, AMD

RÉSUMÉ

La thérapie rétinienne sélective (TRS) est un nouveau procédé laser pour les maladies rétiniennes que l'on suppose être liées à une dégradation de l'épithélium pigmentaire rétinien (EPR). Le but de l'irradiation est d'endommager sélectivement l'EPR sans affecter la rétine neurale, les photorécepteurs et la choroïde. L'objectif du traitement est de stimuler la migration et la prolifération des cellules de l'EPR dans les zones irradiées en vue d'améliorer le métabolisme au niveau des sites rétiniens affectés. Dans une étude pilote, plus de 150 patients atteints d'un épaississement diffus, de rétinopathie séreuse centrale (RSC) et d'œdème maculaire ont été traités. Le premier essai international tricentrique vise l'œdème maculaire diabétique et l'occlusion des branches veineuses.

.....

[1] *Medical Laser Center Lübeck, Germany*
[2] *University Eye Clinic Kiel, Germany*

Dans ce compte-rendu, des effets sélectifs de l'EPR sont mentionnés et deux procédures permettant d'obtenir des effets sélectifs de l'EPR seront introduits: un mode de balayage à ondes pulsées et un mode de balayage à ondes continues. Le mécanisme provoquant les effets sélectifs de l'EPR sera décrit en examinant les résultats *in vitro* et les calculs de température. Ainsi une TRS clinique est menée en appliquant des trains de 30 impulsions laser à partir d'un laser Nd:YLF (527 nm, 1.7 μs, 100 Hz) au niveau des zones affectées. Dans la gamme de 450 à 800 mJ/cm^2 par impulsion, des anomalies de l'EPR ont été constatées de manière angiographique par une fuite de la fluorescéine ou du vert d'indocyanine. La sélectivité par rapport aux tissus adjacents hautement sensibles et l'intervalle de sécurité du traitement seront examinés. Avec les paramètres laser utilisés, ni saignement ni scotome, ceci prouvé par micropérimétrie, n'ont été observés, ce qui indique ainsi l'absence d'effets indésirables sur la choroïde et les photorécepteurs, respectivement. Pendant et après l'irradiation, il est démontré que les locations irradiées sont invisibles d'un point de vue ophtalmoscopique, les effets étant très limités et confinés à l'EPR, ainsi un contrôle de la dosimétrie est requis. Nous décrivons une technique optoacoustique non invasive en ligne permettant de contrôler l'irradiation réussie de l'EPR et de comparer les données avec celles obtenues avec une angiographie standard une heure après le traitement.

MOTS-CLÉS

Traitement sélectif, EPR, impulsions μs, dosimétrie en ligne, scanner laser, DMLA

INTRODUCTION

Laser photocoagulation of the retina has been performed for more than 30 years and is well established for various retinal diseases. Most commonly used are laser wavelengths in the green spectral range (Ar^+-Laser: 514 nm, Nd-Laser: 532 nm), however, also red and near IR-wavelengths are customary. Irradiation is performed typically with a power of 50-300 mW applied over a time 50-300 ms per treated area/spot. The main absorber of the light at the fundus is the retinal pigment epithelium (RPE), which is heavily loaded with strong light absorbing melanosomes (Fig. 1). With the irradiation parameters irreversible thermal denaturation is induced to the RPE [3,56] and owing to heat flow from the RPE into the surroundings also to the choroid and the inner and outer segments of the retina.[56] The power and time of the laser irradiation is adjusted by the ophthalmologist to produce a gray or whitish retinal lesion, originating from increased light scattering indicating tissue denaturation at the irradiation site. The grayish lesions are also regarded as a visible endpoint of a successful photocoagulation and thus serve as a dosimetry control.

Following laser photocoagulation, the targeted tissue undergoes a healing process. Typically, the tissue in the target area will be replaced by proliferating glial tissue originating from the surrounding retina and choroid. RPE cells also contribute significantly to this healing process.[58] It has been shown in animal experiments that the RPE responds in several ways after injury. RPE cells adjacent to the irradiation site may spread out and cover the defect by hypertrophy of neighboring RPE cells.[9,43] The division of RPE cells has also been shown after photocoagulation in rabbits,[24] in monkeys after retinal detachment,[24] and in rabbits after surgically induced RPE defects.[23] The outer blood retinal barrier is normally restored after about 7 days.[25] Further, Glaser has shown that RPE cells produce inhibitors for neovascularization, suggesting that these cells may play a role in the regulation of new vessel growth.[20] In addition, Boulton et al. found significant change of growth factors in the vitreous after panretinal photocoagulation.[4] Yoshimura et al. showed that photocoagulated RPE cells produce inhibitors of endothelial cells.[61] The molecular and immunologic characteristics of these inhibitors correlate with the TGF-β_2. Regenerating RPE cells are known to produce more TGF-β_2 compared to normal RPE cells.[34]

The benefit of retinal laser photocoagulation in various diseases has traditionally been attributed to the destruction of retinal tissue. However, the exact biological effect and the physiological

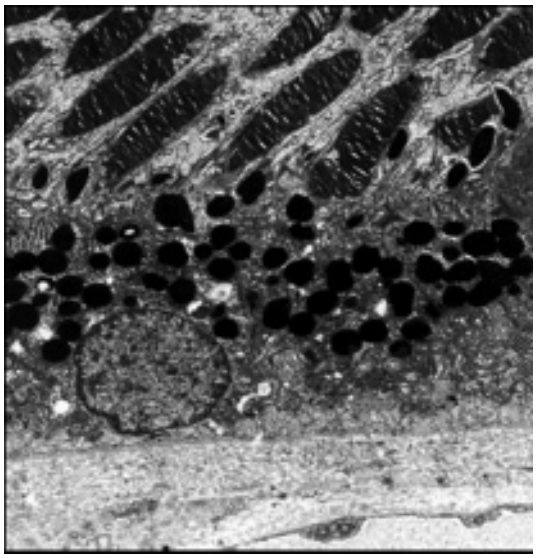

Fig. 1. Transmission electron microscopy (TEM) of a human RPE cell in its environment.[18]

improvement leading to the desired therapeutic effect after this locally severe retinal damage is poorly understood.
In the treatment of diabetic macular edema, the beneficial effect is thought to be mediated by the restoration of a new RPE barrier.[5] A similar effect can be postulated in the treatment of drusen which are located within Bruch's membrane or beneath the RPE and often disappear after photocoagulation of the nearby tissues, eventually likely as a byproduct of surrounding phagocytosis. The efficacy of drusen treatment was studied by several investigators.[14,16] However, since the drusen are located below the retina, there is no clear rationale to routinely include the neural retina in the photocoagulation. The same arguments may count generally in the treatment of macular edema. For instance, in central serous retinopathy (CSR) the rationale of therapy is the photocoagulation and subsequent formation of a new metabolically improved RPE barrier. Here, the simultaneous destruction of the photoreceptors can be regarded as an unwanted side effect. The most common explanation for the beneficial effect of photocoagulation in diabetic retinopathy is the destruction of oxygen consuming photoreceptors.[59] However, another theory suggests that the beneficial effect results from the restoration of a new RPE barrier. The subsequent production of a variety of growth factors [33,60-61] results in an improved RPE metabolism and improved pump function to resolve the edema.

CONCEPT OF SELECTIVE RETINA TREATMENT (SRT)

For a variety of retinal diseases, especially those which are thought to be associated with a degradation of the RPE, it might be sufficient to selectively damage the RPE while the adjacent photoreceptors, the neural retina and the choroid can be spared and thus scotoma be avoided.[44] This is especially useful and demanded within the macular area. If the damaged RPE is rejuvenated in the healing process due to migration and proliferation of the adjoining RPE, such a minimal destructive selective RPE treatment might be optimal for therapy.
The question arises if and how selective RPE effects can be performed. The concept of selective targeting of naturally or artificially pigmented cells or organelles in less strong absorbing surroundings was introduced by Anderson and Parrish [1,38] and led to a variety of applications in ophthalmology [29,43] and dermatology [38] using pulsed laser radiation. Selective cell effects are most interesting in cases where highly sensitive cells, which have to be preserved, are close to the target cells. In this case, a basis for selective RPE damage can be found in the strong light absorbing melanosomes inside the RPE cells, which absorb about 50 % of the incident light in the green spectral range [19] and thus are the dominant chromophores within the fundus of the eye. If laser pulses are applied with pulse durations shorter then the time needed for the produced heat to diffuse, locally confined high temperatures can be obtained at the absorber site. The so-called thermal relaxation time τ_R can be estimated for a spherical particle of radius r and the thermal diffusivity κ to $\tau_R = r^2/4\kappa$. For a melanosome of a radius r = 0.5 μm, the thermal relaxation time $\tau_{R(mel)}$ is calculated to $\tau_{R(mel)} \approx 420$ ns using the thermal diffusivity of water, $\kappa = 1.5 \times 10^5$ $\mu m^2/s$. In order to confine high temperatures to the whole RPE cell with a thickness of approximately 5 μm, $\tau_{R(RPE)} \approx 10$ μs is estimated.
In order to verify such rough estimations for an RPE cell containing multiple discrete absorbers, mathematical models have been developed allowing a more detailed analysis of the spatial and temporal temperature distribution at the fundus of the eye.[2,22,40-41,44] Figure 2 gives the calculated temperature profile inside the RPE and in 5 μm distance at the photoreceptor level. It shows the temporal temperature profile as calculated after a laser exposure with an argon laser, a repetition rate of 500 Hz with single pulse durations of 5 μs.[44] It is conceivable that most of the heat is now concentrated within the RPE at the end of the laser pulse. High temperature peaks only occur within the RPE, highest temperatures are found at and around the single melanin granules. The peak temperature increases proportional with the pulse energy. Due to heat dif-

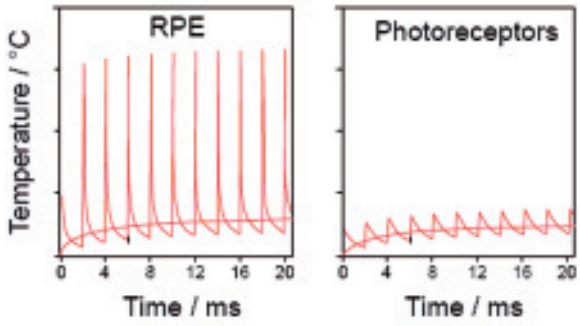

Fig. 2. Transient temperature profile within the RPE and at the photoreceptors (5 μm distance) when applying a train of μs-laser pulses with a repetition rate of 500 Hz, after Roider.[44]

fusion from volumetrically small particles, the peaks are almost cancelled out at just 5 μm distance.[44] On the other hand, the average or background temperature increase at the retina is almost as high as in the RPE. Generally the background temperature depends on the pulse energy and repetition rate, thus the average laser power, and on the overall dimensions of the irradiated area. The ratio of peak to average temperature can be maximized if repetitive short laser pulses are applied in such a manner that the following laser pulse is applied only after the retinal tissue has had sufficient time to completely cool down to baseline. If the peak temperature achieved by one or multiple pulses is high enough to cause damage inside the RPE and the average temperature is low enough to avoid retinal photocoagulation, selective RPE effects should be possible.

APPLICATION MODES FOR SRT

The easiest approach to achieve high peak temperatures is to apply appropriate laser pulses via a commonly available laser slit lamp to the retina. However, if the selective effects in the RPE only rely on these local high temperatures within the RPE cells,[6] this goal should also be obtainable when rapidly scanning a continuous wave (cw) laser beam across the fundus. An arbitrary irradiation pattern can be either generated with one pulse (or repetitive pulses) of a certain pulse duration or it can be obtained by scanning a small laser spot once (or repetitively) across the same area with such a speed, that each point is illuminated for the same time as in the pulsed mode.

In figure 3, the two possible application modalities are sketched exemplary for circular spots assuming an illumination time of 1.7 μs. A pulse duration of 1.7 μs in the pulsed mode corresponds to an application with a scanned 18 μm spot using a speed of 10.6 m/s. For this illumination time, a temperature increase of 100 °C at the surface of a RPE-melanosome requires a radiant exposure of about 310 mJ/cm^2. This corresponds to a pulse energy of 62 μJ for a 160 μm spot or a laser power of 460 mW for an 18 μm spot scanned across the fundus, respectively.[7] Advantages and disadvantages as well as details for both SRT techniques and application modalities (slit lamp vs. fundus camera) are extensively discussed in the literature.[8] In general, the higher flexibility of the scanning approach to easily generate arbitrary pattern geometries competes with its more complicated set-up and application.

THRESHOLD IRRADIATION FOR RPE CELL DAMAGE

In order to investigate thresholds of RPE damage in the range of pulse durations within the thermal relaxation time of the RPE, two different laser systems in the ns to μs time regimen were used for the pulsed mode: a Q-switched, pulse-stretched Nd:YLF laser with adjustable pulse duration between 250 ns and 3 μs at a wavelength of 527 nm and a Q-switched, frequency

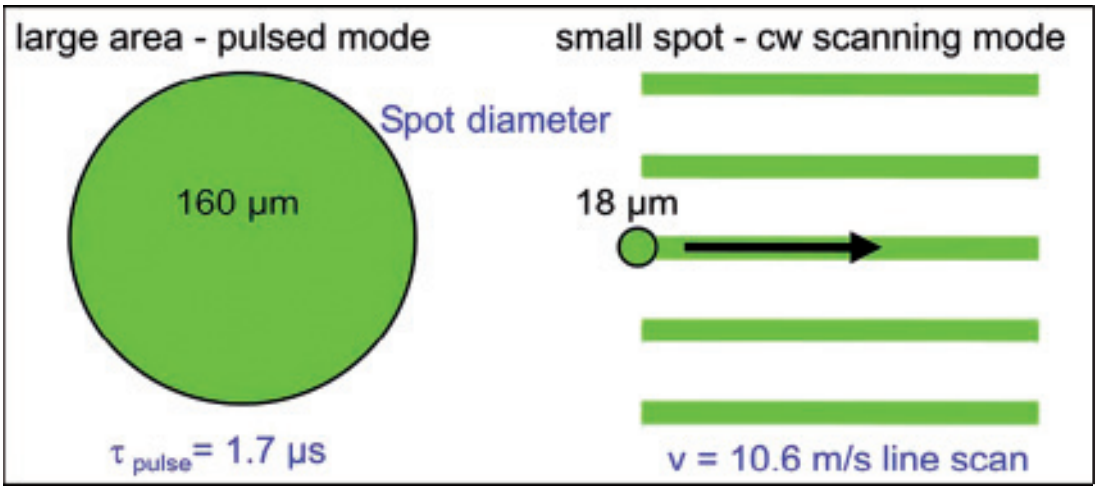

Fig. 3. Possible application modes to achieve µs-laser exposure:[7] either applying laser pulses to a large area with a certain pulse duration (e.g. 1.7 µs) or scanning a continuous wave laser beam across the target area (e.g. 18 µm in diameter with a speed of 10.6 m/s, which gives the same exposure time to each point on the target).

doubled Nd:YAG laser at a wavelength of 532 nm and 8 ns exposure time.[6] For the scanning mode, the beam of an Ar^+-laser was scanned across the probes.[8] Freshly harvested porcine RPE samples served as model. RPE cell vitality prior and after irradiation was probed by the fluorescent dye marker Calcein-AM (Molecular Probes Inc.).[6]
Figure 4 shows the equivalent dose for 50 % cell damage (ED_{50}) radiant exposure for different repetitive exposures to the RPE in the pulsed and scanned mode. When the RPE is irradiated with a train of µs-pulses at a pulse repetition rate of 500 Hz, a decrease of the threshold radiant exposure with the number of pulses applied is observed. With a 40 % drop at 100 pulses, the decrease is most pronounced at a pulse width of 3 µs. The threshold is mostly reduced during the first 500 pulses. Using longer pulse series, the damage threshold almost remains constant. Applying 10 scanned exposures, a threshold power of P_{th} = 569 mW was found, which results in an ED_{50} radiant exposure of H_{th} = 297 mJ/cm^2.[8] The threshold strongly decreases to H_{th} = 131 mJ/cm^2 when applying 500 scans, while a higher number of scans does not lead to a further threshold decrease in accordance with the pulsed application mode. It shows that the threshold radiant exposure is generally higher in the scanning mode, depending on the number of repetitive exposure. Possible reasons for these slight deviations are extensively discussed in the literature.[8] Anyway, both modes show a saturation with higher number of exposures.

ORIGIN OF CELL DAMAGE

The origin of RPE cell damage for repetitive µs laser pulse exposure has extensively been investigated and shall briefly be reviewed. The idea of selective RPE damage has been published by Roider assuming a pure thermal cell damage.[44] It refers to cell and protein denaturation and thus cell necrosis due to the high temperature peaks within the RPE-cell as shown in figure 2. According to the thermal damage model of Arrhenius [2] the rate of damage increases linearly with time and exponential with temperature and is additive for repetitive temperature increase, thus repetitive exposure should be favorable. Further, according to a thermal model, µs-pulse durations in the range of the thermal relaxation time allow to obtain a certain temperature increase for a long time while still having strong temperature decrease towards the retina. However, with respect to the experimental results, the saturation of the threshold radiant exposure as shown in figure 4 is in contradiction to a pure thermal damage, which predicts a continuous

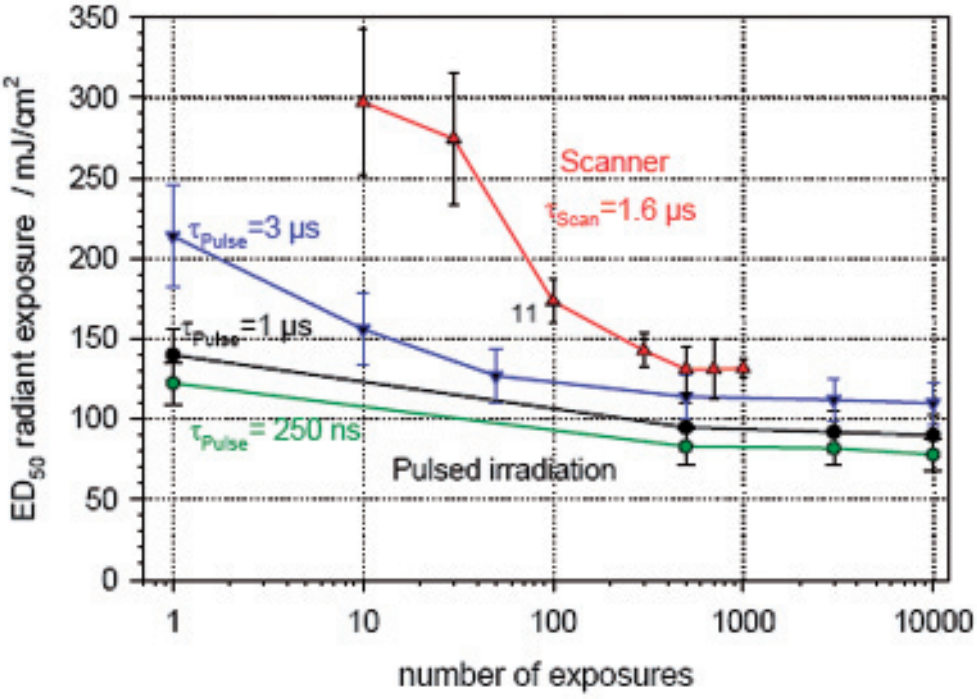

Fig. 4. RPE ED_{50} radiant exposures as a function of number of exposures for the scanned mode (upper curve) [8] and the pulsed mode with pulse durations of 0.25, 1 and 3 μs according to Brinkmann,[6] respectively.

decrease towards higher pulse numbers. Further, a strong dependence of the threshold radiant exposure on the pulse duration below or close to thermal confinement does only exist at the melanosomes directly. Already at small distances apart, the temperature profile does mostly reflect the energy absorbed but less the pulse duration. Thus, at least for the immediate cell damage observed here or in angiography, other mechanisms have to be taken into account. RPE cell damage due to stress waves was investigated in vitro by Douki et al. They found that cell damage is rather dependent on the stress rise time, as on the peak stress, and requires stress transients around 70 bar/ns.[10] However, these pressure gradients can only be achieved with pulse durations close to acoustic confinement conditions, which is below 1 ns for melanosomes.

Apart from these effects, a thermo-mechanical damage of the cells has to be taken into account: Lin and Kelly heated micro absorbers in suspension with ps and ns laser pulses and demonstrated vaporization around the particles.[31] A threshold radiant exposure for micro bubble formation around bovine melanosomes was found to be 55 mJ/cm^2 at a wavelength of 532 nm. Irradiating RPE cells with the same radiant exposure, non-viable cells were only found, when intracellular bubble formation occurred.[26] It was concluded that cell death is caused by thermo-mechanical disruption of the cell structure due to the significantly increased cell volume during bubble lifetime. However, in the highly sensitive retina, strong photo disruptive effects have to be avoided in order to absolutely prevent choroidal disruption, which might lead to bleeding.

We investigated micro bubble formation around isolated porcine melanosomes by fast flash photography as shown in figure 5 and found threshold radiant exposures for bubble formation and cell death to be very close.[6,35] Further both thresholds increase with pulse durations up to 3 μs. Experiments and calculations showed that the temperature for the onset of vaporization at the surface of isolated melanosomes is around 140 °C.[6] This vaporization temperature is higher then the boiling temperature of water under normal conditions, since the formation of micro bubbles

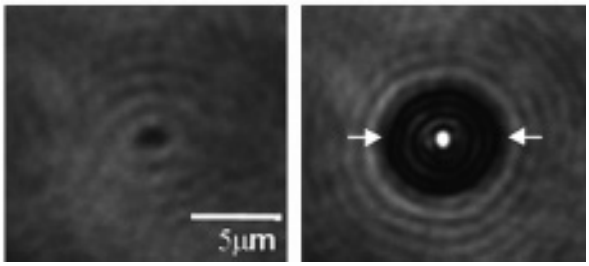

Fig. 5. Fast flash photographs of a melanosome before irradiation (left) and at the half of the bubble lifetime (right, bubble boundary is marked by white arrows). Irradiation with a 12 ns laser pulse (532 nm) at 369 mJ/cm^2 (right) [36].

at or around the melanosomes requires to overcome the surface tension of the bubble, which corresponds to a pressure of approximately 3 bars for a diameter of 1 μm.[6,27]
In another study, we investigated RPE cell damage with a vitality stain up to pulse durations of 3 ms while simultaneously observing microvaporisation.[53] It shows that pressure waves generated by micro bubble formation can very well be measured with hydrophones. Analyzing the acoustic transients allows distinguishing between pressure waves induced by micro bubble formation and by thermo-elastic expansion. This further allows using this opto-acoustic approach as an on-line dosimetry control for SRT as discussed below.
Summarizing, the most probable effect for cell damage up to pulse durations of 50 μs is micro bubble induced photo disruption. When laser pulses with appropriate energy are applied to RPE cells, highest temperatures are induced in and around the melanosomes. If the vaporization temperature of the intracellular plasma is reached, which takes place first at the surface of the melanosomes, micro bubbles begin to form here. Due to the simultaneous growth of a high number of micro bubbles, the cell volume transiently increases, most likely disrupting the cell structure. Using 6 μs pulses, Roegener et al. observed RPE micro bubbles by reflectometry and demonstrated cell damage occurring only if at least in one pulse out of the whole pulse train bubbles were induced.[42]

SUITABLE LASER PARAMETER FOR SRT

Assuming micro bubble formation as the predominant damage mechanism in the ns to μs time regimen, the question arises for the most suitable pulse duration for SRT. For selective RPE damage one has to be also concerned about safety of the highly sensitive photoreceptors and neural retina at the one and the choroid on the other side. Both should neither be harmed by heat nor by photo disruption such as bubble and pressure effects. In order to prove the extension of the thermo mechanical effects with pulse energy and duration we observed bubble lifetime and growth with an interferometer setup.[36] Porcine RPE melanosomes in suspension were irradiated with ns and μs pulses of frequency doubled, Q-switched Nd:YAG and Nd:YLF lasers, respectively. Simultaneously, bubble lifetime was observed by continuous wave HeNe probe laser light (633 nm) deflected by the bubbles and bubble dynamics with an interferometer setup. Exemplary bubble extension was recorded by fast flash photography with a N_2-Dye laser pulse (< 4 ns) and a video microscope.
In the case of ns irradiation the bubble size increases with radiant exposure (Fig. 6, on the left). In the case of 1.8 μs pulses, increasing radiant exposure leads to an earlier onset of bubble formation relative to the laser pulse, whereas the lifetime of the bubble remains nearly constant (Fig. 6, on the right). Further, bubble oscillation is observed and the number of bubbles during the pulse increases. Between two bubbles an off time can be observed.
Analyzing the results more closely, a linear relationship between bubble size, observed by flash photography, and lifetime is obtained for both pulse durations used in this experiment. All data

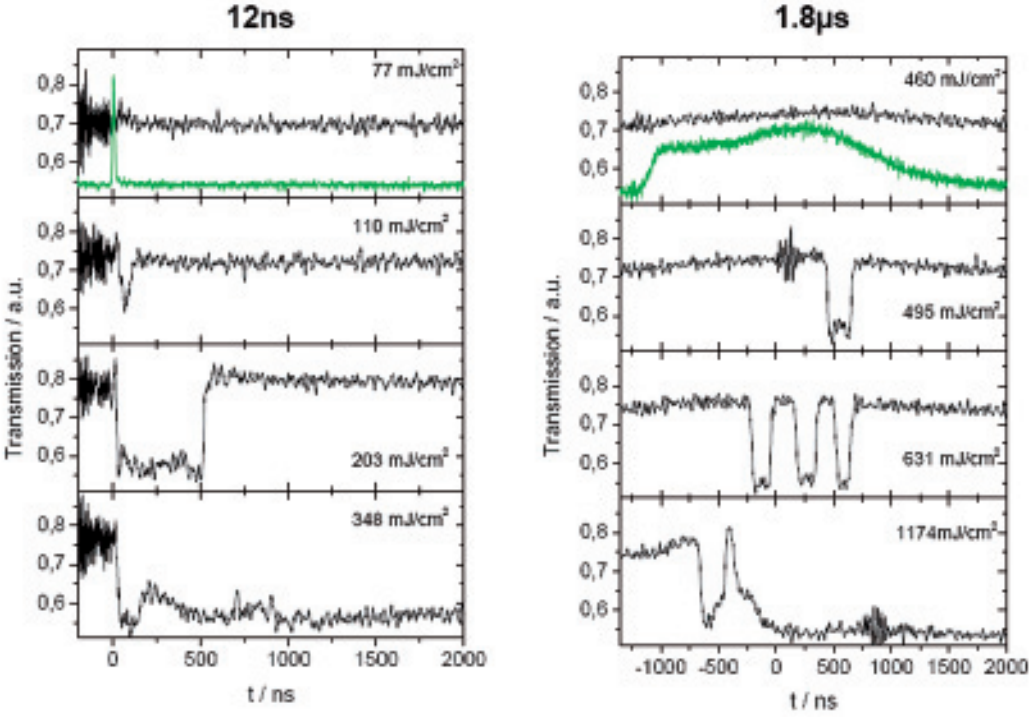

Fig. 6. Time plot of bubble induced deflection of probe laser light for pulse durations of 12 ns (left) and 1.8 μs (right) with increasing radiant exposure (top to bottom). The green pulses show the laser pulse. The duration of dips in the transmitted probe intensity refer to the lifetime of the bubble.[36]

fit the Rayleigh equation, which is known from inertia limited bubble growth,[39] within an interval of ± 20 %. Bubble lifetimes of 250 and 500 ns correspond to a maximum bubble diameter of 1 and 2 μm, respectively. The mean threshold radiant exposures for bubble nucleation are H_{12ns} = 120 ± 28 mJ/cm^2 and $H_{1.8\mu s}$ = 620 ± 159 mJ/cm^2. All data were collected from many individual melanosomes. For the ns-exposure, the maximum bubble size correlates with the pulse energy, while for μs-exposure the onset of bubble formation depends on the pulse energy, its dynamics on the pulse duration.

For SRT, it is recommended to use μs-laser pulses close to threshold in order to keep the selectivity and to avoid the formation of large bubbles and thus the risk of photo disruption of the retina (scotoma) or the choroid (bleeding). Repetitive pulse application is recommended since the threshold radiant exposure for cell damage decreases as shown in figure 4, and thus the pulse energy can be reduced.

SELECTIVITY OF TREATMENT

The questions arise, if such selective RPE damage without harming the photoreceptors and the choroid can be achieved in vivo, and how large the safety regime is with respect to pulse energy until adverse tissue effects occur. The selective damage of the RPE in vivo has first been demonstrated by Roider in rabbits by using 10-500 Ar^+-laser pulses of 5 μs in duration at a repetition rate of 500 Hz.[43] Fluorescein angiography was accomplished to visualize RPE defects. It shows that the treated areas close above threshold for fluorescein leakage were ophthalmoscopically invisible directly after treatment as well as in the follow up period. Two weeks after treatment the lesions were recovered by RPE. Four weeks post treatment a morphologically completely

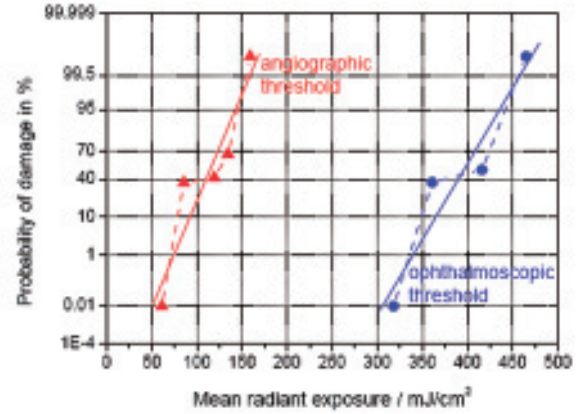

Fig. 7. Angiographic and ophthalmoscopic damage probability for Nd:YLF-laser exposure (wavelength: 527 nm, 100 pulses applied with a repetition rate of 500 Hz) in rabbits with a pulse duration of 1.7 μs on a retinal spot of 102 μm in diameter[15]. Laser irrdiation was performed in five eyes with completely 137 spots. From the linear fit, the 50 % probabilities are obtained: $ED_{50,opht.}$ = 391 mJ/cm^2, $ED_{50,ang.}$ = 113 mJ/cm^2.

restored RPE barrier showing normal RPE cells was found.[43] The selectivity of damage to RPE cells sparing the photoreceptors was demonstrated by histological examinations at different times after treatment.

Further in vivo experiments were conducted to explore the angiographic and ophthalmoscopic ED_{50} threshold radiant exposures over pulse duration in rabbits in more detail.[15] First of all, we explored the thresholds by means of a commonly used Argon$^+$-laser with an irradiation time of 200 ms. Angiographic and ophthalmoscopic thresholds were obtained at 165 W/cm^2 and 205 W/cm^2, respectively. Thus, a small window to achieve solely RPE damage seemed feasible. However, Roider also found different ophthalmoscopic and angiographic thresholds, which differed by a factor of 2 for long pulse irradiation with a 514 nm argon laser (50 ms, 100 ms, 500 ms and 1 s), but histological findings nevertheless revealed destruction of the choroid and the photoreceptors.[43]

With respect to μs exposure times, Fig. 7 shows exemplary the probabilities of angiographic and ophthalmoscopic damage for a pulse duration of 1.7 μs over the peak radiant exposure in rabbits. The angiographic threshold decreases towards shorter pulse duration from 189 mJ/cm^2 (5 μs) to 143 mJ/cm^2 (1,7 μs) and 97 mJ/cm^2 (200 ns), respectively. A comparable decrease over pulse duration was also found for RPE damage in vitro using a vitality stain to prove cell damage, as shown in figure 4.[6] The threshold decrease is expected and can be explained with heat diffusion during irradiation towards longer pulses, since thermal confinement is lost and thus higher pulse energy is needed to reach the vaporization threshold.

The described monotonic increase of the angiographic threshold with pulse duration was not observed for the ophthalmoscopic thresholds. The ED_{50}-thresholds ranged from 478 mJ/cm^2 (1,7 μs), 362 mJ/cm^2 (5 μs) to 438 mJ/cm^2 (200 ns) showing no significant correlation with the pulse duration. A reason could be a higher inaccuracy to determine the whitening of the retina. It is also known that during the first hour after irradiation a biological enhancement of the laser effect, e.g. due to occurrence of an intra- or intercellular edema appears.[32] This might lead to difficulties to judge an opthalmoscopically visible laser lesion, especially for lesions applied with just small energies.

For SRT it is important to have an adequate threshold radiant exposure ratio between ophthalmoscopic and angiographic thresholds, so called "selective window" to prevent surrounding tissue damage. Because of the intra- as well as the inter individual pigmentation, which varies by a factor of 2 in healthy humans [19] and most likely more in diseased areas, a factor of at least 2

must be ensured for safe clinically treatment without dosimetry control. Damage of Bruch's membrane by short pulses should also be avoided because it is known that new vessel formation can be promoted.[11,30]
Referring to the rabbit data we found a decreasing threshold ratio with increasing pulse duration as expected. The ED_{50} threshold ratio for a pulse duration of 1.7 μs is 3.3.[15] However, this ratio is reduced to a factor of about 2 when taking into account the safety ratio between the ED_{99} angiographic and ED_1 ophthalmoscopic threshold. For all parameters used we never found ruptures or hemorrhages below the ED_{86} ophthalmoscopic threshold. However, histological evaluations have to prove whether no extensive mechanical rupture, due to fast bubble extension, lead to a photoreceptor damage. Such damage might not necessarily be ophthalmoscopically visible. The data give a fundamental basis towards appropriate settings for selective RPE treatment, however, the threshold data and ratios for selectivity in rabbits can not simply be transferred to the human retina. Thus, careful clinical investigations were needed as discussed in the following paragraph.

SELECTIVITY OF SRT WITH RESPECT TO AVOID SCOTOMA

In the pilot study, test laser lesions were used to investigate whether sparing of the retina was possible in the human retina.[46] To investigate whether the RPE effects were really selective, microperimetry was performed on 17 patients operating the Nd:YLF laser (527 nm) with a pulse duration of 1.7 μs and a repetition rate of 500 Hz, either applying 100 or 500 pulses per treatment spot. Out of 179 test lesions, 73 were followed at various time steps up to one year follow up by performing microperimetry directly on top of the laser lesions. For testing, the laser lesions threshold stimuli were determined before laser exposure. The threshold sensitivity values were defined as the minimal contrast at which a response was obtained. This threshold value was used for evaluating the test lesions in the follow-up period.
None of the laser effects were visible by ophthalmoscopy during or directly after SRT, while fluorescein angiography clearly demarked the lesions. One day after treatment, retinal defects could be detected in up to 73 % of the patients treated with 500 pulses at 100 μJ. Most of these defects were no longer detectable after three months. After exposure with 100 pulses no defects could be found with 70 and 100 μJ after one day and the neural retina remained undamaged in the follow-up period.[46,48]
The onset of thermal damage after applying 500 pulses with 500 Hz can be attributed to a strong increasing background temperature, which does not only depend on the pulse energy, it also increases with higher pulse repetition rate and larger spot diameter due to reduced heat diffusion.[2] In order to avoid high average temperature increase during irradiation, we irradiated all patients, apart from the very first ones, with just 100 pulses at a repetition rate of 500 Hz on a retinal spot of 160 μm. In the ongoing multicenter trial we slightly increased the spot diameter to 200 μm, but therefore reduced the pulse repetition rate to 100 Hz. In order to avoid eye movements during treatment, the irradiation time was limited to 300 ms, referring to 30 pulses per spot.
The microperimetry findings impressively demonstrate the selectivity after SRT in contrast to conventional laser photocoagulation. Laser photocoagulation is associated with thermal damage of the outer and inner nuclear layer and replacement by scar tissue.[45,57-58] It is not surprising that such lesions lead to absolute scotoma on microperimetry, which can be detected over each argon laser exposure. If such lesions are located temporal to the fovea the patient might become reading problems, despite a good visual acuity.

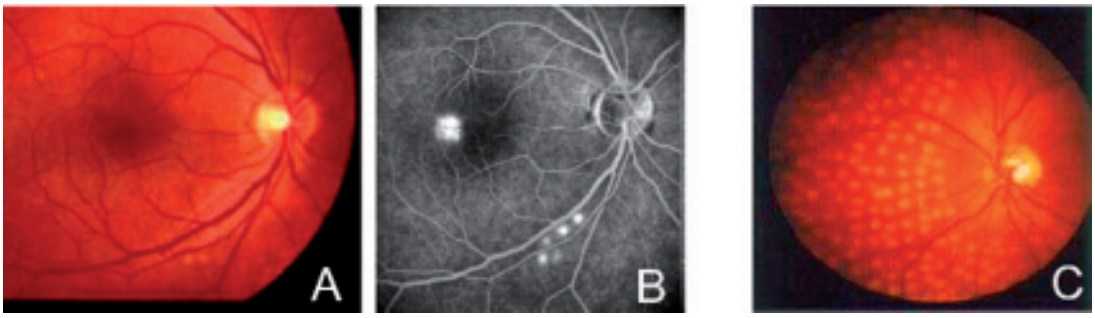

Fig. 8. Fundus picture (A) and fluorescein angiogram (B) of an CRS patient. SRT lesions clearly show up in angiography.[50] Test lesions for dosimetry were performed in the arcades, only highest pulse energies lead to a slightly visible effect. Treatment was performed in the macular area with pulse energies leading just to an angiographically visible effect. For comparison to standard photocoagulation, (C) shows a fundus appearance after panretinal photocoagulation.[21]

FIRST CLINICAL RESULTS

A salient question is whether and in which diseases selective RPE treatment might lead to a positive therapeutic effect. In a first clinical study we focused on three pathological conditions: diabetic macular edema, central serous retinopathy, and drusen in age related macular degeneration (AMD). Twelve patients with diabetic maculopathy (group I), ten with soft drusen (group II) and four with central serous retinopathy (CSR) (group III) were treated and followed up for one year.[47]

SRT was performed with a self developed frequency doubled, pulse stretched Nd:YLF laser (wavelength 527 nm, pulse duration 1.7 μs).[6] Either 30 laser pulses per area with a repetition rate of 100 Hz or 100 pulses at 500 Hz, respectively, were applied on a spot diameter of 160 μm. Angiographically visible lowest radiant exposures were found between 350-500 mJ/cm^2 per pulse in test expositions at the arcades to prove for individual dosimetry among different patients. For the treatment typically 650 mJ/cm^2 were used, in order to compensate for the variation in pigmentation and ocular transmission.

Patients were examined at various times after treatment by ophthalmoscopy, fluorescein- and ICG angiography as well as infrared imaging. After six months in group I hard exsudates disappeared in 6 out of 9, and leakage disappeared in 6 out of 12 diabetic patients. In group II drusen were less in 7 out of 10 patients. In group III serous detachment disappeared in 3 out of 4 cases. Visual acuity was stable in all cases.

SRT MULTICENTER TRIAL

Because of the promising pilot study results, an international SRT multicenter trial has been started to evaluate the therapeutic effect of SRT in patients with diabetic maculopathy and in patients with macular edema after venous branch or central venous occlusion. Further few patients with geographic atrophy secondary to AMD and patients with occult CNV secondary to AMD are treated at single locations. Study centers are at the university eye clinics in Lübeck and Kiel and the St. Thomas Hospital in London.

So far, more than 60 patients with diabetic maculopathy were treated and controlled 6 months after treatment. In 95 % of the patients the visual acuity was improved or stable at the 6 month follow-up control. The angiographic results with respect to leakage areas and Optical Coherence Tomography (OCT) data with respect to edema size and thickness however don't show fully consistent with respect to the visual acuity.

Further remarkable are the treatment of 10 patients with central serous rethinopathy (CSR) with a persisting edema for at least three month. For this pathology the results are very impressive.

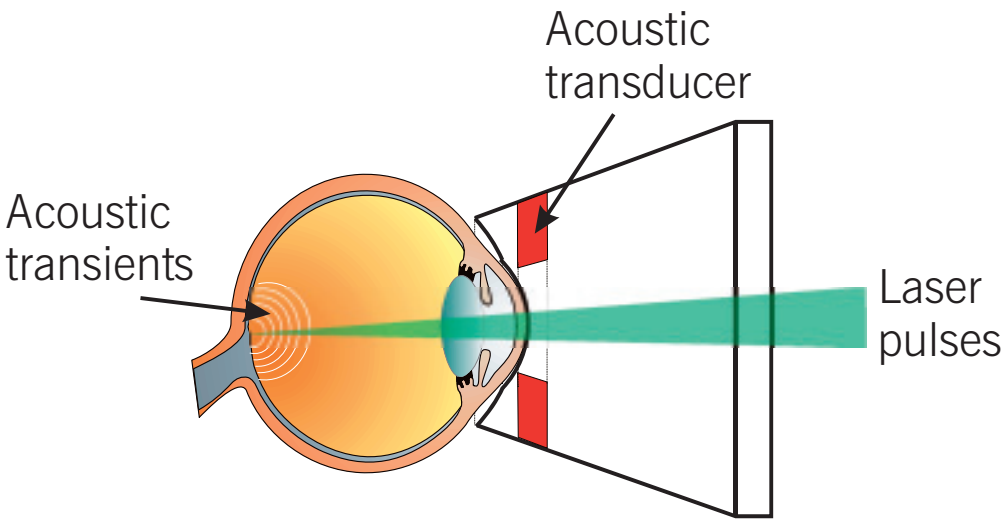

Fig. 9. Contact lens with integrated ultrasonic pressure wave detector, after Schüle.[49]

All treated patients showed a complete disappearance of subretinal fluid after 4 weeks and 9 out of 10 patients demonstrated a significant increase in visual acuity after 3 months. These results suggest to change the standard recommendation for treating CSR patients. SRT offers the possibility of treating CSR and DMP patients much earlier in the course of the disease.

ON-LINE DOSIMETRY

The formation of microbubbles around the strong absorbing melanosomes inside the RPE has been identified as the leading mechanism of RPE damage during μs laser pulse exposure.[7,53] Mechanical effects such as cell disruption from a large number of simultaneously forming intracellular microbubbles most likely induce the RPE cell damage. If a correlation between fluorescein leakage and microbubble formation can be demonstrated, than the detection of microbubbles enables an on-line dosimetry control avoiding test lesions and thus additional angiography.

If energy is absorbed and converted to heat, the thermoelastic expansion of the absorbing medium as a matter of principle leads to the emission of a bipolar pressure wave.[54-55] Optoacoustic (OA) techniques have been used in ophthalmology for imaging of the ciliary body. OA monitoring of transscleral cyclophotocoagulation is possible in vitro.[37] It can further be used to determine the background RPE/retinal temperature increase during SRT.[51] Using probe laser pulses it also enables for the first time to determine non-invasively on-line the temperature increase during cw photocoagulation and during transpupillary thermo therapy (TTT), which could already be demonstrated in vitro. Further OA techniques are used for temperature mapping in tissue during laser induced thermo therapy (LITT).[12-13, 28]

Strong OA transients are also induced at the RPE during μs laser irradiation.[51] After exceeding the vaporization threshold, additional transients will be emitted owing to the formation and collapse of multiple microbubbles.[49] Due to the μs heating and cooling and to the μs bubble lifetime, both thermo-elastic and bubble induced pressure transients are expected in the ultrasonic MHz frequency range.

By use of an ultrasonic needle hydrophone, we measured pressure in vitro during μs-laser exposure of the RPE.[49,51] In order to non-invasively detect the acoustic transients during patient treatment a standard contact lens was modified with an ultrasonic transducer, as sketched in figure

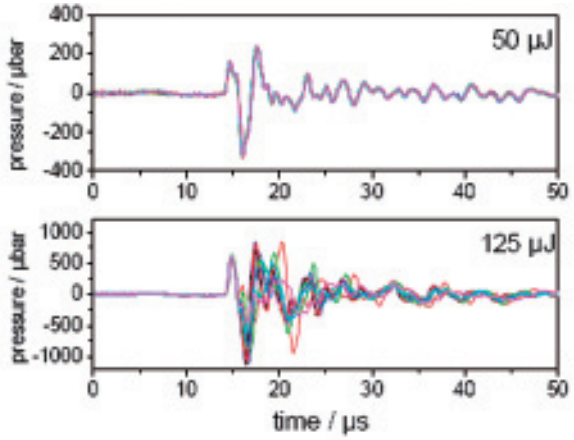

Fig. 10. Typical pressure transients from patient treatment: 30 pulses of one pulse train super-imposed, respectively.[51] (A) Spot showing no RPE leakage, (B) Spot showing RPE leakage

9. With a transducer well adapted to the expected frequency range and amplitudes we were able to detect pressure amplitudes on-line during SRT.

Figure 10 displays typical superpositions of the 30 OA transients from each pulse of a pulse train as recorded with the contact lens, referring to two pulse energies and locations within one patient's eye. For exposures which result in no angiographic visible lesion (Fig. 10 A, 50 μJ) the 30 OA transients show a clear reproducible bipolar thermoelastic pressure transient originating from thermal expansion of the heated RPE. The pressure amplitudes are around 0.3 mbar. At higher exposures (Fig. 10 B, 125 μJ, spot was angiographically visible) a stronger thermoelastic bipolar transient is measured. Moreover, small pulse-to-pulse fluctuations start after the first pressure peak most likely resulting from the statistic bubble formation and expansion. The delay to the thermoelastic wave originates from the previous heating of the tissue and corresponds to the optically detected bubble onset delay (Fig. 6). All treatment spots were ophthalmoscopically invisible.

A mathematical algorithm was derived to separate the fluctuations from the thermo-elastic background.[51] The algorithm gives a number which is related to the maximal pressure differences between thermoelastic and bubble transients, the so-called OA-value. The analysis was limited to a temporal window from 12 to 30 μs. Within this time frame most fluctuations appear.

ANGIOGRAPHIC RPE LEAKAGE VERSUS OPTOACOUSTIC ON-LINE DOSIMETRY

Roider and Birngruber introduced angiographic determined fluorescein or ICG-leakage without ophthalmoscopically visible effects as reference for selective RPE damage. In order to prove whether the detection of microbubble formation correlates to angiographic findings, every single laser spot was analyzed with respect to its OA-value and angiographic response. The first study was limited to four RCS patients, because due to the diffuse FLA leakage at the fundus in patients with diabetic maculopathy a direct comparison of every single treatment spot was not possible. In figure 11 all analyzed OA-values of these four treatments are plotted over the pulse energy used. The open symbols mark all angiographically visible lesions, filled gray symbols the FLA negative and filled black symbols the data points, which were not angiographically analyzable. A threshold for OA detectable angiographic lesion can be defined as OA = 1.96 10^{-10} bar $\times$ s. In case of these four treatments two out of 94 lesions were detected as false/positive and two as false/negative. The OA threshold for an angiographic lesion during patient treatment of

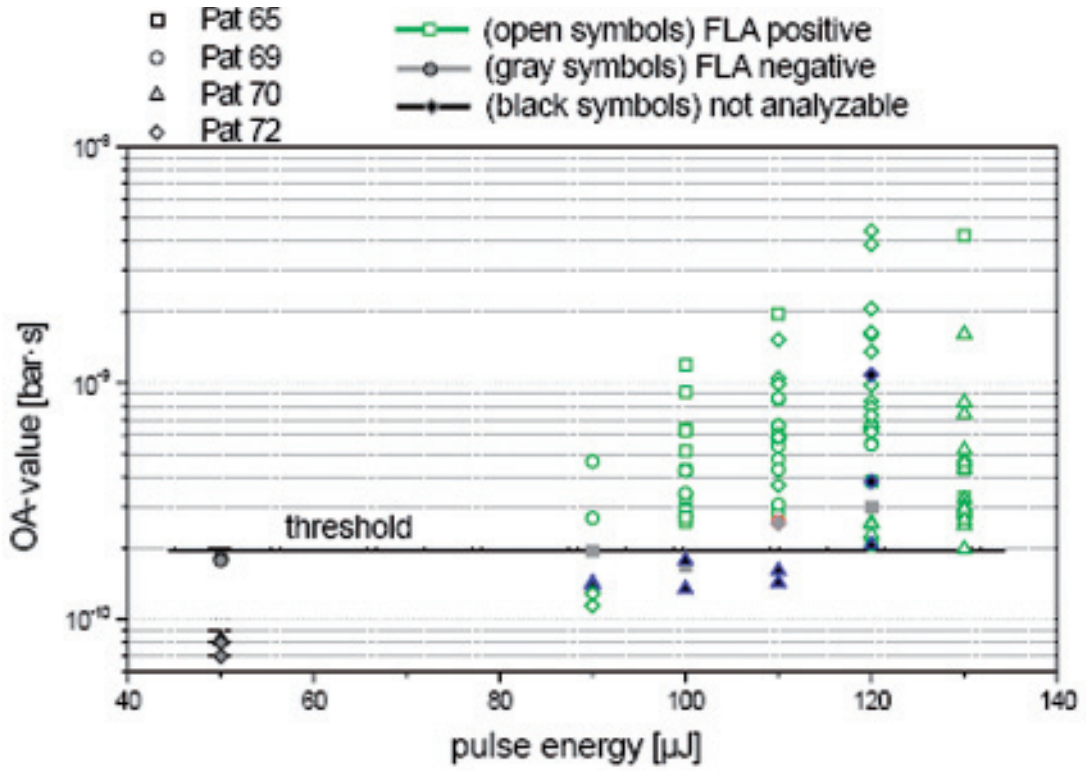

Fig. 11. OA-value over applied pulse energy of four different CRS patient treatments. The open symbols mark the FLA positive lesions, gray symbols FLA negative and the black symbols not analyzable data points.[51]

OA = 1.96 10^{-10} bar × s is very close to the threshold of porcine RPE damage in vitro of OA = 2.4 10^{-10} bar × s.[51]

By carefully conducting in vitro experiments it could be demonstrated that the extracted OA-value increased with the number of damaged cells within one spot.[52] However, due to the limited optical resolution, the amount of damaged RPE cells cannot be directly analyzed in a patient. Therefore, we plotted the OA-values measured for each spot and allocated them in figure 12. Roughly the brightness of the spot increases with increasing OA-value, which might give a hint for an increasing RPE damage. However, a quantitative analysis of the cell damage is impossible with current techniques. Future investigations using ultra high-resolution OCT [17] in combination with adaptive optics might lead to the demanded resolution to quantify RPE damage and to follow the healing response in patients.

In summary we proved that the concept of an OA-based non-invasive online dosimetry control for SRT is feasible. As well in vitro on porcine RPE samples as during SRT, the OA dosimetry system enables to detect the laser induced RPE damage. The OA dosimetry system is currently embedded in the multicenter clinical SRT study in order to control dosimetry, and is further evaluated with respect to angiographic correlations.

ACKNOWLEDGEMENT

The authors like to thank Jörg Neumann and Dirk Theisen-Kunde from MLL, Georg Schüle (Lumenis Inc, Santa Clara, CA), Carsten Framme (University Eye Clinic, Regensburg, Germany), Hanno Elsner (University Eye Clinic, Kiel, Germany), Peter Hamilton (St. Thomas Hospital, Lon-

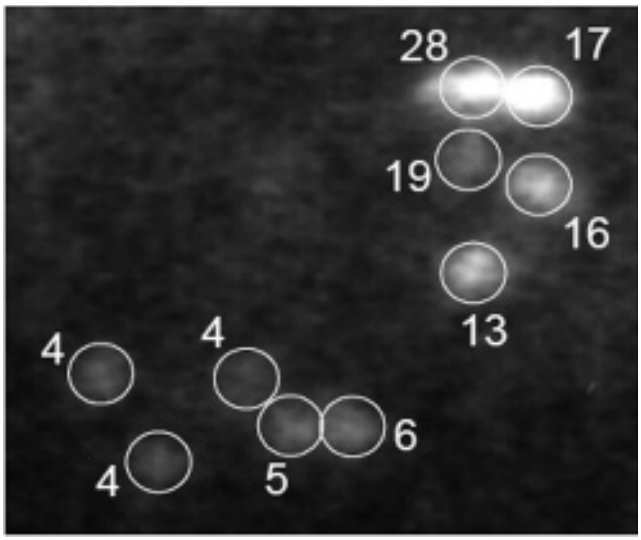

Fig. 12. ICG-angiogram of different SRT spots. Numbers given are the determined OA-values ($\times 10^{-10}$ bar $\times$ s).[62]

don, Great Britain), Clemens Alt and Charles P. Lin (Wellman Center of Photomedicine and Harvard Medical School, Boston, USA) for their participation in the various parts of the SRT project.

REFERENCES

(1) ANDERSON R.R., PARRISH J.A. – Selective Photothermolysis: Precise Microsurgery by Selective Absorption of Pulsed Laser Radiation. Science 1983; 220: 524-527
(2) BIRNGRUBER R. – Thermal modeling in biological tissue. In: Hillenkamp, Pratesi, Sacchi (eds.) Lasers in Biology and Medicine. Plenum Press, New York 1980; 77-97
(3) BIRNGRUBER R., HILLENKAMP F., GABEL V.P. – Theoretical investigations of laser thermal retinal injury. Health Phys. 1985; 48: 781-796
(4) BOULTON M.E., M X., KHALIQ A., MORIARTY P., J C., D M. – Changes in growth factor expression in pig eyes following scatter laser photocoagulation. Invest Ophthalmol Vis Sci 1995; 36 (Suppl.): 95
(5) BRESNICK G.H. – Diabetic maculopathy: A critical review highlighting diffuse macular edema. Ophthalmology 1983; 90: 1301-1317
(6) BRINKMANN R., HÜTTMANN G., RÖGENER J., ROIDER J., BIRNGRUBER R., LIN C.P. – Origin of retinal pigment epithelium cell damage by pulsed laser irradiance in the nanosecond to microsecond time regimen. Lasers Surg Med 2000; 27 (5): 451-464
(7) BRINKMANN R., KOOP N., ÖZDEMIR M., ALT C., SCHÜLE G., LIN C.P., BIRNGRUBER R. – Selective damage of pigmented cells by means of a rapidly scanned cw laser beam. Proc SPIE 2002; 4617: 134-140
(8) BRINKMANN R., KOOP N., ÖZDEMIR M., ALT C., SCHÜLE G., LIN C.P., BIRNGRUBER R. – Targeting the Retinal Pigment Epithelium (RPE) by Means of a Rapidly Scanned Continuous Wave (CW) Laser Beam. Lasers Surg Med 2003; 32 (4): 252-264
(9) BÜLOW N. – The process of wound healing of the avascular outer layers of the retina. Light- and electron microscopic studies on laser lesions of monkey eyes. Acta Ophthalmol (Copenh) 1978; 139 (Suppl.): 7-60
(10) DOUKI T., LEE S., DOREY K., FLOTTE T., DEUTSCH T., DOUKAS A.G. – Stress-Wave-Induced Injury to Retinal Pigment Epithelium Cells In Vitro. Lasers Surg Med 1996; 19: 249-259
(11) ELDIRINI A.A., OGDEN T.E., RYAN S.J. – Subretinal endophotocoagulation: A new model of subretinal neovascularisation in the rabbit. Retina 1991, 11, 244-249
(12) ESENALIEV R.O., ORAEVSKY A.A., LARIN K.V., LARINA I.V., MOTAMEDI M. – Real-time optoacoustic monitoring of temperature in tissues. Proc SPIE 1999; 3601: 268-275

(13) ESENALIEV R.O., LARINA I.V., LARIN K.V., MOTAMEDI M. – Real-time optoacoustic monitoring during thermotherapy. Proc SPIE 2000; 3916: 302-310
(14) FIGUEROA M.S., REGUERAS A., BERTRAND J., APARICIO M.J., MANRIQUE M.G. – Laser photocoagulation for macular soft drusen. Retina 1997; 17 (5): 378-384
(15) FRAMME C., SCHÜLE G., ROIDER J., KRACHT D., BIRNGRUBER R., BRINKMANN R. – Threshold determinations for selective RPE damage with repetitive microsecond laser systems in rabbits. Ophthalmic surg las 2002; 33 (5): 400-409
(16) FRENNESSON C., NILSSON. – Significant decrease in exsudative complications after prophylactic laser treatment of soft drusen maculopathy in a randomized study. Invest Ophthalmol Vis Sci 1997; 38 (4 Suppl): 18
(17) FUJIMOTO J.G. – Optical coherence tomography for ultrahigh resolution in vivo imaging. Nat Biotechnol 2003; 21 (11): 1361-1367
(18) GABEL V.P. – Die Lichtabsorption am Augenhintergrund. Habilitation Ludwig-Maximilians Universität München 1974
(19) GABEL V.P., BIRNGRUBER R., HILLENKAMP F. – Visible and near infrared light absorption in pigment epithelium and choroid. Congress Series: XXIII Concilium Ophthalmologicum 1978; 450: 658-662
(20) GLASER B.M., CAMPOCHIARO P.A., DAVIS J.L., JERDAN J.A. – Retinal pigment epithelial cells release inhibitors of neovascularization. Ophthalmology 1987; 94: 780-784
(21) GREHN F. – Augenheilkunde. Springer Verlag, Berlin - Heidelberg - New York 1998
(22) HAGENAU R., BRINKMANN R. – Simulation of laser treatment on scalable parallel computer architectures. In: Jähnichen S., Zhou X. (eds.) The fourth international workshop on advanced parallel processing technologies. Ilmenau 2001; 137-146
(23) HERIOT W., MACHEMAR R. – Pigment epithelial repair. Graefe's Arch Clin Exp Ophthalmol 1992; 230: 91-100
(24) INOMATA H. – Wound healing after xenon arc photocoagulation in the rabbit retina. Ophthalmologica (Basel) 1975; 170: 462-474
(25) JOHNSON R.N., MCNAUGHT E.I., FOULDS W.S. – Effect of photocoagulation on the barrier function of the pigment epithelium. II. A study by electron microscopy. Trans Ophthalmol Soc UK 1977; 97: 640-651
(26) KELLY W.M., LIN C.P. – Microcavitation and cell injury in RPE cells following short-pulsed laser irradiation. Proc SPIE 1997; 2975: 174-179
(27) KUCHLING H. – Taschenbuch der Physik. Fachbuchverlag, Leipzig 1996; 16 (Auflage)
(28) LARIN K.V., LARINA I.V., MOTAMEDI M., ESENALIEV R.O. – Monitoring of temperature distribution in tissues with optoacoustic technique in real time. SPIE 2000; 3916: 311-321
(29) LATINA M.A., PARK C. – Selective Targeting of Trabecular Meshwork cells: In Vitro Studies of Pulsed and CW Laser Interaction. Exp Eye Res 1995; 60: 359-372
(30) LEWIS H., SCHACHAT A.P., HAIMAN M.H., HALLER J.A., QUINLAN P., VON FRICKEN M.A., FINE S.L., MURPHY R.P. – Choroidal neovascularization after laser photocoagulation for diabetic macular edema. Ophthalmology 1990; 97: 503-511
(31) LIN C.P., KELLY M.W., SIBAYAN S.A.B., LATINA M.A., ANDERSON R.R. – Selective Cell Killing by Microparticle Absorption of Pulsed Laser Radiation. IEEE J select Topics Quantum Electron 1999; 5 (4): 963-968
(32) LORENZ B. – Morphologic changes of chorioretinal argon laser burns during the first hour post exposure. In: Welch (ed.) Lasers in the life sciences, Vol. 2. Harwood Acad Publ, Chur, London 1988; 207-226
(33) MARSHALL J., CLOVER G., ROTHERY S. – Some new findings of retinal irradiation by krypton and argon lasers. In: Birngruber, Gabel (eds.) Laser treatment and photocoagulation of the eye. Junk Publ (Vol Doc Ophthalmol Proc Series), The Hague 1984; 36
(34) MATSUMOTO M., YOSHIMURA N., HONDA Y. – Increased production of transforming growth factor-β2 from cultured human retinal pigment epithelial cells by photocoagulation. Invest Ophthalmol Vis Sci 1994; 35: 4645-4652
(35) NEUMANN J., BRINKMANN R. – Interferometric detection of laser-induced microbubbles in the retinal pigment epithelium. In: Birngruber R., Van den Bergh H. (eds.) Laser-Tissue Interactions, Therapeutic Applications, and Photodynamic Therapy. Proc SPIE 2001; 4433: 81-86
(36) NEUMANN J., BRINKMANN R. – Microbubble dynamics around laser heated microparticles. Proc SPIE 2003; 5142: 82-87

(37) OBERHEIDE U., BRUDER I., WELLING H., ERTMER W., LUBATSCHOWSKI H. – Optoacoustic imaging for optimization of laser cyclophotocoagulation. J Biomed Opt 2003; 8 (2): 281-287
(38) PARRISH J.A., ANDERSON R.R., HARRIST T., PAUL B., MURPHY G.F. – Selective Thermal Effects with Pulsed Irradiation from Lasers: From Organ to Organelle. J Invest Derm 1983; 80 (6): 75-80
(39) PLESSET M.S., PROSPERETTI A. – Bubble Dynamics and Cavitation. Ann Rev Fluid Mech 1977; 9: 145-185
(40) PUSTOVALOV V.K. – Thermal processes under the action of laser radiation pulse on absorbing granules in heterogeneous biotissues. Int J Heat Mass Trans 1993; 36: 391-399
(41) PUSTOVALOV V.K., KHORUNZHII I.A. – Theoretical consideration of the selective thermodenaturation of pigment epithelium layer using short laser pulses. Proc SPIE 1994; 2126: 111-115
(42) ROEGENER J., BRINKMANN R., LIN C.P. – Pump-probe detection of laser-induced microbubble formation in retinal pigment epithelium cells. J Biomedical Optics 2004; 9 (2): 367-371
(43) ROIDER J., MICHAUD N.A., FLOTTE T.J., BIRNGRUBER R. – Response of the Retinal Pigment Epithelium to Selective Photocoagulation. Arch Ophthalmol 1992; 110: 1786-1792
(44) ROIDER J., HILLENKAMP F., FLOTTE T.J., BIRNGRUBER R. – Microphotocoagulation: Selective effects of repetitive short laser pulses. Proc Nat Acad Sci USA 1993; 90: 8463-8647
(45) ROIDER J., MICHAUD N., FLOTTE T., BIRNGRUBER R. – Histologie von Netzhautläsionen nach kontinuierlicher Bestrahlung und nach selektiver Mikrokoagulation des retinalen Pigmentepithels. Ophthalmologe 1993; 90: 274-278
(46) ROIDER J., BRINKMANN R., WIRBELAUER C., LAQUA H., BIRNGRUBER R. – Retinal sparing by selective retinal pigment epithelial photocoagulation. Arch Ophthalmol 1999; 117: 1028-1034
(47) ROIDER J., BRINKMANN R., WIRBELAUER C., LAQUA H., BIRNGRUBER R. – Subthreshold (retinal pigment epithelium) photocoagulation in macular diseases: a pilot study. Br J Ophthalmol 2000; 84: 40-47
(48) ROIDER J., BRINKMANN R., BIRNGRUBER R. – Selective retinal pigment epithelium laser treatment. Theoretical and clinical aspects. In: Fankhauser, Kwasniewska (eds.) Lasers in ophthalmology: basic, diagnostic and surgical aspects. Kugler Publications, The Hague 2003; 119-129
(49) SCHÜLE G., HÜTTMANN G., ROIDER J., WIRBELAUER C., BIRNGRUBER R., BRINKMANN R. – Optoacoustic measurements during μs-irradiation of the retinal pigment epithelium. Proc SPIE 2000; 3914: 230-236
(50) SCHÜLE G. – Mechanismen und On-line Dosimetrie bei selektiver RPE Therapie (dissertation, Medizinische Universität zu Lübeck) 2002
(51) SCHÜLE G., HÜTTMANN G., FRAMME C., ROIDER J., BRINKMANN R. – Non-invasive optoacoustic temperature determination at the fundus of the eye during laser irradiation. J Biomedical Optics 2004; 9 (1): 173-179
(52) SCHÜLE G., ELSNER R., FRAMME C., ROIDER J., BIRNGRUBER R., BRINKMANN R. – Optoacoustic real-time dosimetry for selective retina treatment. J Biomed Opt 2005; 10: 1-11
(53) SCHÜLE G., RUMOHR M., HÜTTMANN G., BRINKMANN R. – RPE damage thresholds and mechanisms for laser exposure in the μs to ms time regimen. Inv Ophthalmol Vis Sci 2005; 46 (2): 714-719
(54) SIGRIST M.W., KNEUBÜHL F.K. – Laser-generated stress waves in liquids. Journal of the Acoustical Society of America 1978; 64 (6): 1652-1663
(55) SIGRIST M.W. – Laser generation of acoustic waves in liquids and gases. J Appl Phys 1986; 60 (7): 85-121
(56) VOGEL A., BIRNGRUBER R. – Temperature profiles in human retina and choroid during laser coagulation with different wavelengths ranging from 514-810 nm. Lasers Light Ophthalmol 1992; 5: 9-16
(57) WALLOW I.H., TSO M.O.M., FINE B.S.F. – Retinal repair after experimental xenon arc photocoagulation. 1. A comparison between rhesus monkey and rabbit. Am J Ophthalmol 1973; 75: 32-52
(58) WALLOW I.H. – Repair of the pigment epithelial barrier following photocoagulation. Arch Ophthalmol 1984; 102: 126-135
(59) WOLBARSHT M.L., LANDERS M.B. – The rationale of photocoagulation therapy for proliferative diabetic retinopathy: A review and a model. Ophthalmic Surg Lasers 1980; 11: 235-245
(60) YAMAMOTO C., OGATA N., X Y., TAKAHASHI K., MIYASHIRO M., YAMADA H., UYAMA M., MATSUZAKI K. – Immunolocalization of transforming growth factor β during wound repair after laser photocoagulation. Graefe's Arch Clin Exp Ophthalmol 1998; 236: 41-46

(61) YOSHIMURA N., MATSUMOTO M., SHIMIZU H., MANDAI M., HATA Y., ISHIBASHI T. – Photocoagulated human retinal pigment epithelial cells produce an inhibitor of vascular endothelial cell proliferation. Invest Ophthalmol Vis Sci 1995; 36: 1686-1691

.....

corresponding address:

Dr. Ralf Brinkmann
University of Lübeck, Institute of Biomedical Optics and
Medical Laser Center Lübeck GmbH
Peter-Monnik-Weg 4, D-23562 Lübeck, Germany
Tel: +49-451-500-6507
brinkmann@mll.mu-luebeck.de

Prof. Dr. med. Johann Roider
University of Kiel and
Clinic of Ophthalmology of the University Clinicum Schleswig-Holstein, Campus Kiel
Hegewischstr. 2, D-24105 Kiel, Germany
Tel: +49-431-597-2360
roider@ophthalmol.uni-kiel.de

Prof. Reginald Birngruber
University of Lübeck, Institute of Biomedical Optics and
Medical Laser Center Lübeck GmbH
Peter-Monnik-Weg 4, D-23562 Lübeck, Germany
Tel: +49-451-500-6501
bgb@mll.mu-luebeck.de